

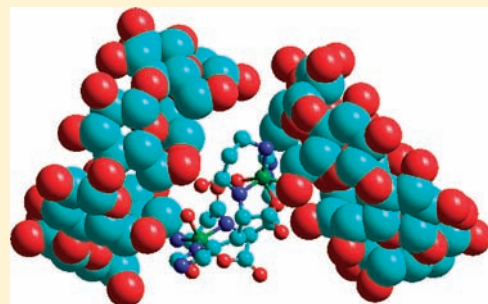
Noncovalent Interaction-Driven Stereoselectivity of Copper(II) Complexes with Cyclodextrin Derivatives of L- and D-Carnosine

Giuseppa Ida Grasso, Francesco Bellia, Giuseppe Arena, Graziella Vecchio,* and Enrico Rizzarelli

Department of Chemistry, University of Catania, Viale A. Doria 6, 95125 Catania, Italy

Supporting Information

ABSTRACT: L-Carnosine (β -alanyl-L-histidine, LCar) is the most widely and abundantly distributed copper(II)-coordinating endogenous dipeptide. Though its physiological role has not been completely understood yet, many functions have been proposed for this compound. LCar might be crucial in the potential reduction or prevention of several pathologies in which the metal ions are thought to be involved. The potential therapeutic applications of LCar are drastically limited because of hydrolysis by specific dipeptidases (carnosinases). D-Carnosine (DCar), the enantiomer of the naturally occurring dipeptide, shows the same properties as those of LCar, but it is not hydrolyzed by carnosinases. Chemical modification of LCar has been proposed as a promising strategy to reduce its enzymatic hydrolysis; conjugation of a carbohydrate moiety may also improve site-specific transport to different tissues, which would enhance the peptide bioavailability. On this basis, we have functionalized DCar with β -cyclodextrin (CDDCar) and characterized the compound via NMR. The copper(II) binding properties of the new DCar derivative were investigated by spectroscopic techniques (UV-vis, circular dichroism, electron paramagnetic resonance) and potentiometric measurements. The results surprisingly revealed a pronounced difference from the analogous LCar derivative (CDLCar), especially concerning the dimeric species. The spectroscopic data show that this stereoselectivity is driven by noncovalent interactions, namely, hydrogen bonds, CH- π interactions, and steric and hydrophobic effects of the cyclodextrin cavity.



INTRODUCTION

The stereoselectivity in the formation of metal complexes with peptide ligands has an important impact in the field of medicinal inorganic chemistry.^{1,2} The metal-ion coordination of small peptides is often directly involved in several biochemical processes. Many papers about the stereoselective formation of transition-metal complexes with oligopeptides have been published in the last 30 years.^{3–5} The metal binding properties of endogenous compounds greatly influence metal homeostasis⁶ (metal homeostasis), and their study may help in the development of clinical approaches for the treatment of metal-involving pathologies.⁷

Carnosine (β -alanyl-L-histidine, LCar), which is found in the muscle and nervous tissues of several animal species, is the most widely and abundantly distributed copper(II)-coordinating endogenous dipeptide.⁸ Though its physiological role is not completely understood yet, carnosine and other histidine-containing dipeptides (homocarnosine and anserine) act in vivo as physiological buffers, wound-healing promoters, ion-chelating agents especially for copper(II) and zinc(II), antioxidants, and free-radical scavengers.^{9,10} It has been proven that carnosine shows antiperoxidative activity on proteins,¹¹ lipids,¹² and DNA;¹³ moreover, it acts as an antioxidant and antiinflammatory agent in lung injury caused by bleomycin administration¹⁴ and ischemia/reperfusion liver injury in rats.¹⁵ Hence, carnosine is widely used for nutraceutical applications.^{16–19}

LCar binding affinity for copper(II) and zinc(II) has been extensively investigated,²⁰ and it might be crucial in the potential reduction or prevention of several pathologies, such as ALS, Alzheimer's, and Parkinson's diseases,^{21,22} in which the two metal ions are thought to be involved.²³ Other types of disorders may also be treated with metal complexes of carnosine. For example, it has been shown that the zinc(II) carnosine complex (polaprezinc) is effective for the repair of ulcers and other gut lesions.^{24,25}

Notwithstanding the beneficial effect of carnosine in several biological processes, its potential therapeutic applications are drastically limited because of hydrolysis by specific dipeptidases, called carnosinases: CN1, the serum-circulating form secreted by brain cells into the cerebrospinal fluid,^{26–28} and CN2, the nonspecific cytosolic isoform, distributed in several human tissues and in rodent brains.^{26,29,30}

The chemical modification of L-carnosine is a promising strategy to reduce its enzymatic hydrolysis,^{31,32} conjugation of a carbohydrate moiety may also improve site-specific transport to different tissues, which would enhance the peptide bioavailability.^{33,34}

Cyclodextrins (CDs) are cyclic chiral oligomers of D-(+)-glucopyranosyl units linked by α -1,4-glycosidic bonds. These molecules are water-soluble and have the shape of a truncated

Received: January 20, 2011

Published: April 22, 2011

cone with a hydrophobic cavity. A number of CD-based conjugates with amines, amino acids, peptides, and aromatic systems have recently been reported.^{35–38} CDs are widely used for drug delivery, as complexing agents, conjugating moieties, stabilizers, and carrier systems of drugs for their controlled release, especially in the colon.^{39–41} Furthermore, CD appropriate functionalization favors metal-ion complexation³⁶ and thus may improve applications of the CD chemistry in the field of chiral recognition and metalloenzyme mimicking.

Recently, carnosine has been conjugated with β -CD,^{42–44} trehalose,⁴⁵ glucose, and lactose.⁴⁶ All of these compounds are able to scavenge hydroxyl radicals, and their copper(II) complexes exhibit SOD-like activity.⁴⁴ Furthermore, they are resistant to the hydrolytic activity of carnosinase⁴⁷ and have an antioxidant effect at concentrations 10–20 times lower than that reported for other synthetic derivatives.⁴⁸

D-Carnosine (DCar), the enantiomer of the naturally occurring dipeptide, is not hydrolyzed by carnosinases, is able to cross the blood–brain barrier, and maintains the same quenching activity as L-carnosine in vitro;⁴⁹ hence, its use has been suggested for the treatment or prevention of oxidative stress-induced disorders.⁵⁰

On the basis of the above considerations, we have functionalized DCar with β -CD (CDDCar) and characterized the compound via NMR. The proton and copper(II) complex formation constants have been determined by means of potentiometric measurements. The spectroscopic investigation [UV–vis, circular dichroism, electron paramagnetic resonance (EPR)] of the metal complex system has highlighted similarities and differences with the analogous CD derivative of the natural dipeptide L-carnosine (CDLCar).

EXPERIMENTAL SECTION

Chemicals. Commercially available reagents were used directly unless otherwise specified.

β -Cyclodextrin (Fluka) was dried under vacuum (10^{-2} mmHg) for 24 h at 80 °C, using a P_2O_5 trap. D-Carnosine was kindly provided by Flamma (Milan), while L-carnosine was purchased from Sigma. Thin-layer chromatography (TLC) was performed on silica gel (60F-254, 0.20 mm, Macherey-Nagel), and the products that were not detectable under UV light were revealed with a 5% solution of anisaldehyde in ethanol (containing 5% H_2SO_4) and Pauli's reagent for peptide derivatives.

Copper(II) nitrate was prepared from copper(II) basic carbonate by adding a slight excess of HNO_3 ; the concentration of stock solutions was determined by ethylenediaminetetraacetic acid titrations using murexide as an indicator.⁵¹

High-purity water (Millipore, Milli-Q Element A 10 ultrapure water) and grade A glassware were employed.

D-Carnosine ethyl ester (DCarOEt) was synthesized from DCar (1.00 g, 4.43 mmol) in ethanol (30 mL) at 0 °C with acetyl chloride (5 mL) as the HCl source. After 2 h, the solvent was evaporated under vacuum, and the crude product was purified using a Sephadex-DEAE-A25 anion-exchange column (20 × 600 mm, HCO_3^- form) and water as the eluent.

Synthesis of 6^A-[(3-[(1R)-1-carboxy-2-(1H-imidazol-4-yl)ethyl]amino)-3-oxopropyl]amino]-6^A-deoxy- β -cyclodextrin (CDDCar). DCarOEt (0.60 g, 2.36 mmol) was added under stirring to the appropriate amount of dry iodide-functionalized CD⁵² (0.60 g, 0.48 mmol) dissolved in *N,N*-dimethylformamide (DMF; 40 mL). The reaction was carried out at 60 °C under nitrogen. After 24 h, DMF was evaporated in vacuo at 40 °C. The yellow syrup obtained was washed with acetone until the acetone remained colorless. The solid

obtained was dissolved in water and precipitated again with acetone. The precipitate collected by suction was dissolved in water, and the solution was passed through a column (45 × 500 mm) of CM-Sephadex C-25 resin (NH_4^+ form). The column was eluted initially with water (800 mL) and then with a gradient from 0 to 0.2 M of aqueous ammonium hydrogen carbonate (4 L, total volume). The collected fractions were assayed by TLC. Fractions that gave only one spot with $R_f = 0.71$ (5:3:1 PrOH/ H_2O/NH_3) were combined and evaporated to dryness at 40 °C in vacuo to eliminate ammonium hydrogen carbonate. The residue was dissolved in water and reprecipitated by using acetone. The product was hydrolyzed by a 1% NaOH solution at room temperature. After 2 h, the solvent was evaporated and the product was purified on a CM-Sephadex C-25 column, using water as the eluent. The collected fractions were combined and evaporated to dryness at 40 °C in vacuo. CDDCar yield: 13%. TLC: $R_f = 0.56$ (5:3:1 PrOH/ H_2O/NH_3). ¹H NMR: δ 8.20 (s, 1H, 2), 7.05 (s, 1H, 4), 5.04 (d, 1H, 1A) 5.00–4.96 (m, 6H, H-1 β -CD), 4.32 (m, 1H, X), 4.04 (m, 1H, 5A), 3.92–3.64 (m, 25H, H-3, H-5, and H-6 of β -CD), 3.60–3.40 (m, 15H, H-2, H-4, 6A), 3.24 (m, 1H, H-6'A), 3.20 (m, 2H, β), 3.10 (m, 1H, a), 2.98 (m, 1H, b), 2.62 (m, 2H, α). ESI-MS: m/z 1343.8 ($M + 1$).

Thermal Analysis. Thermogravimetric analysis of the ligand was carried out using a Perkin-Elmer TGS-2 instrument. Typically, samples (ca. 2 mg) were heated from 50 to 800 °C under a nitrogen-controlled atmosphere (heating rate 10 °C min^{-1}).

Electromotive Force (EMF) Measurements. Potentiometric titrations were performed with two home-assembled fully automated apparatus sets (Metrohm E654 pH-meter, combined micro pH glass electrode, Orion 9103SC, Hamilton microlab 500 series dispenser) controlled by the appropriate software set up in our laboratory.

The titration cell (2.5 cm^3) was thermostatted at 25.0 ± 0.2 °C, and all solutions were kept under an atmosphere of argon, which was bubbled through a solution having the same ionic strength and temperature as the measuring cell.

KOH solutions (0.1 $mol\ dm^{-3}$) were added through a Hamilton buret equipped with 1 cm^3 syringes. The system was calibrated on the $pH = -\log [H^+]$ scale by titrating HNO_3 with CO_2 free base. The values of E^0 , E_p , K_w , and the Nernstian slope of the electrodic system were determined in separate experiments by titrating nitric acid with CO_2 -free sodium hydroxide. The ionic strength of all solutions was adjusted to 0.10 $mol\ dm^{-3}$ (KNO_3).

In order to determine the stability constants, solutions of the ligand (protonation constants) or the ligand + Cu^{2+} (copper complex constants) were titrated with 0.1 $mol\ dm^{-3}$ sodium hydroxide. The ligand concentration ranged from 2.4 to 4.0×10^{-3} and from 3.4 to 4.2×10^{-3} $mol\ dm^{-3}$ for the protonation and complexation experiments, respectively. A minimum of three independent runs were performed to determine the protonation constants, while eight independent experiments were run for the copper(II) complexation constants. An excess of ligand was used in order to avoid precipitation of the copper hydroxy species: Cu^{2+} /ligand ratios ranged from 0.8 to 0.9, with each run comprising 85–95 points. The initial pH was always adjusted to 2.4. To avoid systematic errors and verify reproducibility, the EMF values of each experiment were taken at different time intervals.

The HNO_3 excess in metal stock solutions was determined by Gran's method.^{53,54} Other details were as previously reported.⁴²

To obtain protonation and complexation constants, the potentiometric data were refined using *Hyperquad*,⁵⁴ which minimizes the error square sum of the measured electrode potentials through a nonlinear iterative refinement of the sum of the squared residuals, U , and also allows for the simultaneous refinement of data from different titrations:

$$U = \sum (E_{exp} - E_{calc})^2$$

where E_{exp} and E_{calc} are the experimental and calculated electrode potentials, respectively.

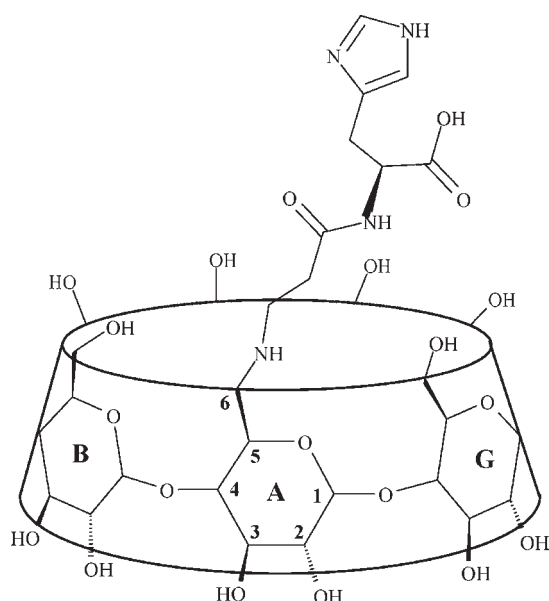


Figure 1. Schematic representation of CDDCar.

The species distribution as a function of the pH was obtained by using the computer program *Hyss* (www.hyperquad.co.uk).

Spectroscopic Measurements. ^1H NMR spectra were recorded at 25 °C in D_2O with a Varian Unity Plus 500 spectrometer at 499.883 MHz. The ^1H NMR spectra were recorded by using the standard pulse programs from the Varian library. In all cases, the length of 90° pulse was ca. 7 μs . The two-dimensional (2D) experiments were acquired using 1K data points, 256 increments, and a relaxation delay of 1.2 s. DSS was used as the external standard. The CDDCar concentration was about 5×10^{-3} M. The pH values were adjusted by DCl or NaOD solutions.

UV–vis spectra of the copper(II) complexes were recorded on a Cary 500 spectrophotometer (Varian) in 1-cm-path-length quartz cells.

Circular dichroism spectra of the ligand and its copper(II) complexes were recorded on a Jasco 810 spectropolarimeter at a scan rate of 50 nm min^{-1} and a resolution of 0.1 nm. The path lengths were 1 or 0.1 cm, in the 190–800 nm range. The spectra were recorded as an average of 10 or 20 scans. Calibration of the instrument was performed with a 0.06% solution of ammonium camphorsulfonate in water [$\Delta\epsilon = 2.40$ ($\text{mol dm}^{-3})^{-1} \text{cm}^{-1}$ at 290.5 nm]. The 200–800 nm spectral range was covered by using quartz cells of various path lengths. The results are reported as ϵ (molar adsorption coefficient) and $\Delta\epsilon$ (molar dichroic coefficient) in $\text{mol}^{-1} \text{dm}^3 \text{cm}^{-1}$.

A Bruker Elexsys E500 continuous-wave EPR spectrometer driven by a PC running an XEPR program under Linux and equipped with a Super X-band microwave bridge operating at 9.3–9.5 GHz and a SHQE cavity was used throughout this work. All spectra were recorded at 150 K using quartz tubes with 3 mm inner diameter. Solutions of $^{63}\text{Cu}(\text{NO}_3)_2$ and the ligand at different molar ratios were prepared in water, containing a small quantity of methanol (<10%) and varying the pH by the addition of potassium hydroxide. The g_{\parallel} and A_{\parallel} values were taken directly from the experimental spectra.

The copper(II) complexes were prepared without adjusting the ionic strength with KNO_3 because it was verified that the salt addition did not modify the spectra.

The parallel spin-Hamiltonian parameters of $[\text{Cu}_2(\text{CDDCar})_2\text{H}_{-2}]$ were calculated using the *GNDIMER* program, which uses the dipole–dipole as the only source of anisotropic coupling between the two Cu^{II} ions.⁵⁵

Molecular Modeling Simulations. Molecular modeling calculations were performed by *Hyperchem 8.0* software (trial edition) in three

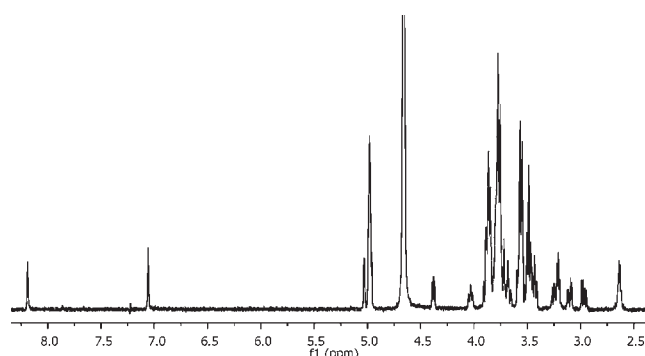


Figure 2. ^1H NMR (D_2O , 500 MHz) of CDDCar (5.0×10^{-3} mol dm^{-3}) at pH 7.

steps. In the first, the atomic charges of the ligands (CDLCar and CDDCar) were calculated (semiempirical method PM3), and the conformational search was used to determine the suitable structure of the molecular systems. In the second step, the ligands were inserted into boxes containing 1500 water molecules and minimized (Molecular Mechanics, Amber force field). Finally, any ligand was coordinated with the metal ion and the resulting dimeric complex species inserted into a box containing 4500 water molecules and minimized (algorithm Polak-Ribiere, conjugate gradient; termination condition = 0.01 $\text{kcal } \text{Å}^{-1} \text{mol}^{-1}$). Several cycles of geometry optimization–molecular dynamics were applied to evaluate the possible presence of local minima in the geometry refinement.

RESULTS AND DISCUSSION

Synthesis and NMR Characterization. 6^A -[(3-((1R)-1-carboxy-2-(1H-imidazol-4-yl)ethyl)amino)-3-oxopropyl]amino-6^A-deoxy- β -cyclodextrin (CDDCar; Figure 1) was synthesized from iodide-functionalized β -CD through nucleophilic substitution. The carboxylic group of D-histidine was protected by esterification with ethanol. The final product was purified by ion-exchange chromatography.

The ^1H NMR spectrum of CDDCar is reported in Figure 2. The signals were assigned by 2D spectra (COSY, TOCSY, HSQC, ROESY; see Figures S1–S12 in the Supporting Information). In addition to the signals due to the CD moiety, the protons of imidazole resonate at 8.20 and 7.05 ppm; the ABX system of histidine resonates at 4.32, 3.47, and 2.97 ppm. The signal due to H-5 is detected at 4.04 ppm. The diastereotopic H-6a and H-6'a protons resonate at 3.50 and 3.24 ppm, as is typically observed for these kinds of derivatives.³⁶ The chemical shift values of H-5 and H-6 suggest that this compound is in its zwitterionic form.⁴² The downfield shifts of the signals due to H-6, H-5, and β - CH_2 in comparison to the spectrum recorded at basic pH suggest the involvement of an amino group in the first protonation spectra. No correlation between the carnosine and the CD moiety is detected in the ROESY spectra, as reported for the CDLCar epimer.⁴²

The NMR spectra carried out at basic and acidic pH do not markedly differ from those reported for the CDLCar epimer. The histidine residue is bound to CD through the β -alanine chain, and no enantiospecific interaction is indicated by the NMR spectra, unlike other similar systems in which the chiral molecule is directly bound to the cavity.⁵⁶

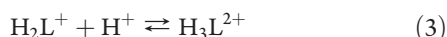
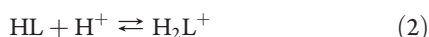
Proton Complex Formation. The protonation equilibria of the ligands are given in eqs 1–3, where L is the anionic form of

Table 1. Stability Constant Values for the Protonation of the Ligands (DCar, CDLCar, and CDDCar) at 25° C and $I = 0.10 \text{ mol dm}^{-3}$ (KNO_3)

equilibrium	group	ligand ^a		
		DCar	CDDCar	CDLCar ⁴²
$\text{L}^- + \text{H}^+ \rightleftharpoons \text{LH}$	amino	9.36(3)	7.83(2)	7.69
$\text{LH} + \text{H}^+ \rightleftharpoons \text{LH}_2^+$	imidazole	6.78(6)	6.63(2)	6.60
$\text{LH}^+ + \text{H}^+ \rightleftharpoons \text{LH}_3^{2+}$	carboxylate	2.58(6)	2.73(3)	2.66

^a 3σ in parentheses.

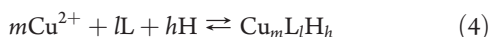
the ligand (DCar or CDDCar).



Analysis of the titration data for DCar and CDDCar provides the protonation constants for the amino and imidazole nitrogen atoms as well as for the carboxylate group. The proton complex formation constant values are given in Table 1; for clarity, we have also reported the groups they refer to.

DCar has the same protonation constant values as those of its enantiomer LCar,⁴² as expected. The CDDCar protonation constants do not differ significantly from those of the analogous L diastereoisomer (CDLCar).⁴² On the contrary, their comparison with those of the parent dipeptide (DCar) shows a significant decrease in the protonation value of the amino group (ca. 1.5 logarithmic units), as reported for other amine–CD derivatives.^{57,58} Small or no changes are observed for protonation of the imidazole and carboxylate groups. The basicity drop of the amino group in the CD derivative results from a smaller enthalpy contribution to its protonation in comparison with that of the free dipeptide, as was found for the analogous trehalose derivatives;⁴⁵ the less favorable enthalpic value might be ascribed to an intramolecular hydrogen bond between the amino group and a CD primary OH group as well as to the steric and hydrophobic effects of the CD cavity.^{42,45}

Copper(II) Complex Formation. The equilibria for the formation of the copper(II) complexes are given in eq 4, where L is the anionic form of the ligand (DCar or CDDCar; the charges of the copper(II) complexes have been omitted for the sake of clarity).



The overall stability constant β_{mlh} is defined by eq 5.

$$\beta_{mlh} = \frac{[\text{Cu}_m\text{L}_l\text{H}_h]}{[\text{Cu}]^m[\text{L}]^l[\text{H}]^h} \quad (5)$$

The experimental titration curves can be satisfactorily fitted by considering the equilibria shown in eqs 6–11.



Table 2. Stability Constant Values for the Copper(II) Complexes of the Ligands (CDLCar and CDDCar) at 25° C and $I = 0.10 \text{ mol dm}^{-3}$ (KNO_3)

equilibrium	ligand ^a	
	CDDCar	CDLCar ⁴²
$\text{Cu}^{2+} + \text{L}^- + \text{H}^+ \rightleftharpoons [\text{CuLH}]^{2+}$	11.42(3)	11.58
$\text{Cu}^{2+} + \text{L}^- \rightleftharpoons [\text{CuL}]^+$	6.36(2)	6.92
$\text{Cu}^{2+} + \text{L}^- \rightleftharpoons [\text{CuLH}_{-1}] + \text{H}^+$		1.3
$2\text{Cu}^{2+} + 2\text{L}^- \rightleftharpoons [\text{Cu}_2\text{L}_2\text{H}_{-2}] + 2\text{H}^+$	3.47(2)	6.33
$2\text{Cu}^{2+} + \text{L}^- \rightleftharpoons [\text{Cu}_2\text{LH}_{-1}] + \text{H}^+$	3.51(6)	
$\text{Cu}^{2+} + \text{L}^- \rightleftharpoons [\text{CuLH}_{-2}] + 2\text{H}^+$	−9.30(2)	

^a 3σ in parentheses.

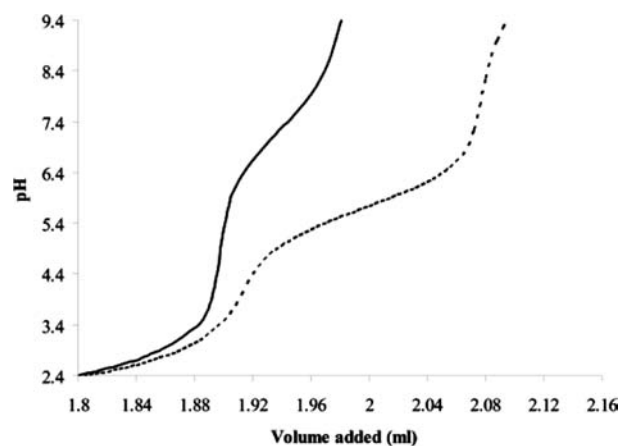
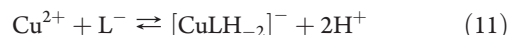
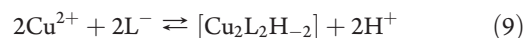


Figure 3. CDDCar protonation curve (continuous line) and proton displacement caused by the presence of copper(II) (broken line).



The stability constant values of the copper(II) complexes of the ligands are reported in Table 2. Typical protonation and copper(II) complexation curves are shown in Figure 3. The large difference between the protonation (continuous line) and complexation (broken line) curves is indicative of a marked extra-proton displacement resulting from the formation of strong copper(II) complexes. The distribution diagrams for the copper complex systems with CDDCar and CDLCar⁴² are reported in Figure 4.

The species distribution of the copper(II) complexes with DCar and LCar⁴² are similar to each other with only minor differences (data not shown). As for protonation, the introduction of the CD moiety modifies the species distribution of the copper(II) complexes of both LCar and DCar. The copper(II) species distribution for CDLCar and CDDCar (Figure 4) shows that CuLH and CuL form up to pH 6.5; the dimer $\text{Cu}_2\text{L}_2\text{H}_{-2}$ is

the main species at physiological pH, and CuLH_{-2} is detected only for the complex system with CDDCar (Figure 4B). The log β values for the $\text{Cu}_2\text{L}_2\text{H}_{-2}$ species of the CD conjugates with LCar and DCar (6.33 and 3.47, respectively; Table 2) differ markedly. The last peculiar difference has also been reported for the analogous derivatives with trehalose,⁴⁵ for which the derivative with DCar is less stable than the analogous diastereoisomer with LCar. However, the marked difference observed for the carnosine dimeric derivatives cannot be explained solely based on the thermodynamic data. To this end, spectroscopy may be of some help because it provides information on the coordination geometry that might originate the difference between the constant values of the dimers.

Spectroscopic Data. The spectroscopic data for the copper(II) complexes of CDDCar are reported in Table 3 together with those of CDLCar.⁴² The complex species were studied at pH values where they reached the maximum of formation (Figure 4).

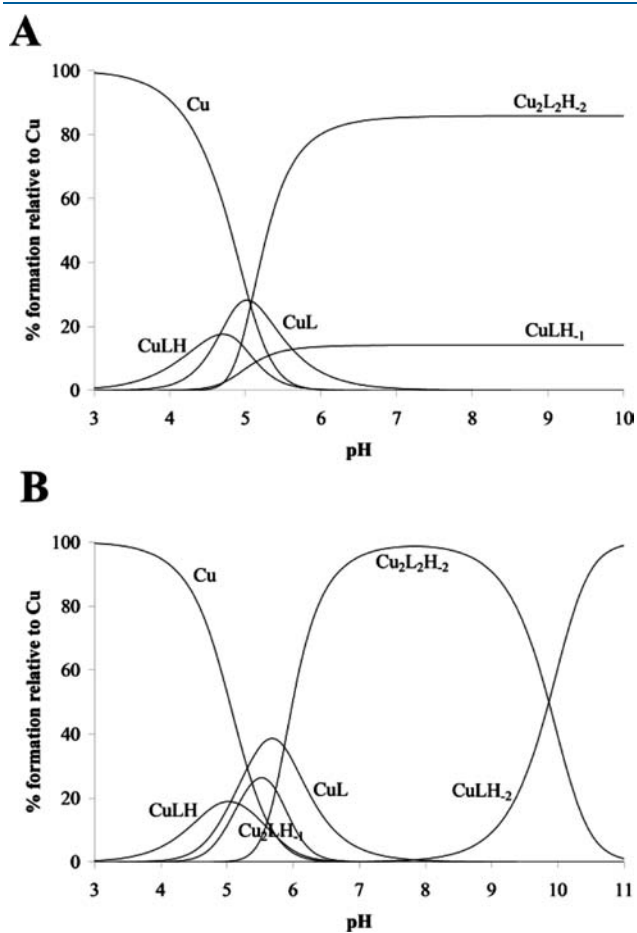


Figure 4. Species distribution diagram for the copper(II)–CDLCar⁴² (A) and the copper(II)–CDDCar (B) systems (1:1.2 metal/ligand; $C_L = 3.5 \times 10^{-3} \text{ mol dm}^{-3}$).

Table 3. Spectroscopic Data for the Copper(II) Complexes of CDDCar and CDLCar⁴²

ligand	pH	UV–vis λ/nm ($\epsilon/\text{M}^{-1} \text{ cm}^{-1}$)	circular dichroism λ/nm ($\Delta\epsilon/\text{M}^{-1} \text{ cm}^{-1}$)
CDDCar	8.0	641 (139)	735 (−0.11), 575 (1.04), 320 (−0.41), 281 (−1.57), 213 (−10.06)
	11.0	631 (137)	591 (0.40), 320 (−0.19), 265 (−0.94), 215 (−7.55)
CDLCar	7.2	644 (142)	715 (0.60), 593 (−2.89), 312 (0.71), 275 (2.60), 215 (19.00)

In the UV–vis spectra at pH 8.0, where $[\text{Cu}_2(\text{CDDCar})_2\text{H}_{-2}]$ is the main species (Table 2), the d–d transition band is red-shifted by 37 nm and the ϵ value is larger than that of copper(II)–DCar. A similar band shift was also reported for the copper(II) complex with CDLCar,⁴² and it was ascribed to the lower ligand-field strength. This effect is also due to the lower basicity of the β -alanine amino group bound to the CD moiety. The λ_{max} (641 nm) and ϵ ($139 \text{ M}^{-1} \text{ cm}^{-1}$) values of the copper(II) complex with CDDCar are very close to those reported for the metal complex with CDLCar ($\lambda_{\text{max}} = 644 \text{ nm}$; $\epsilon = 142 \text{ M}^{-1} \text{ cm}^{-1}$).

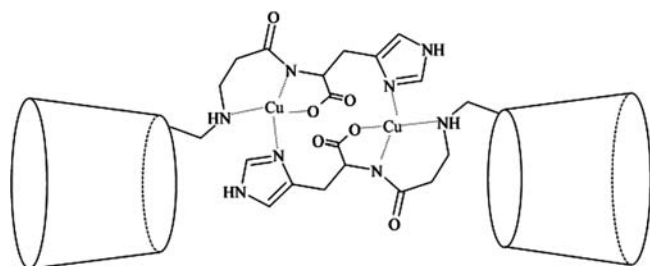
The dichroic bands of the dimeric species of CDDCar and CDLCar (Table 3) are similar in terms of λ_{max} and the absolute value, while they have opposite signs. Thus, the dichroic bands of the copper(II) complex with CDDCar may be assigned by analogy with the analogous complex with the diastereoisomer CDLCar.⁴² The $n \rightarrow \pi^*$ transition of the carbonyl chromophore and the $\pi \rightarrow \pi^*$ transition of the imidazole ring are responsible for the dichroic band at 213 nm. The bands centered at 281 and 320 nm can be assigned to the charge-transfer transition from the amino group and the deprotonated amide to Cu^{2+} , respectively, while those at 575 and 735 nm give the same signals as those detected in the copper(II)–DCar spectra and are to be ascribed to the d–d transition. The greater Cotton effect of the copper(II)–CDDCar complex with respect to that of DCar is in keeping with the data reported for similar systems,³⁶ for which such a difference was ascribed to the CD cavity. Thus, the UV–vis and circular dichroic parameters for the $\text{Cu}_2\text{L}_2\text{H}_{-2}$ species suggest the same coordination geometry for both copper(II) complex systems.

The EPR spectrum (X band) of a frozen (77 K) aqueous solution containing an equimolar concentration of Cu^{2+} and CDDCar at pH 7.5 exhibited a $\Delta m = 1$ transition resolved into a seven-line pattern with apparent intensities of 1:2:3:4:3:2:1 and a peak-to-peak width of about 80 G. This pattern results from the coupling of the two copper(II) nuclei ($I = 3/2$) involved in the dimeric species. EPR simulation for the copper(II)–CDDCar dimer was carried out to determine the magnetic parameters (Table 4). The values of the analogous copper(II) dimeric species with CDLCar are also reported for comparison.⁴²

The EPR spectra for $[\text{Cu}_2(\text{CDDCar})_2\text{H}_{-2}]$ show values ($g_{\parallel} \geq g_{\perp} \geq 2.04$) that are typical for axial copper(II) complexes having coordination geometries with $d_{x^2-y^2}$ ground state. The A_{\parallel} and g_{\perp} values for $[\text{Cu}_2(\text{CDDCar})_2\text{H}_{-2}]$ are slightly smaller and larger, respectively, than those of the analogous species with CDLCar, while g_{\parallel} values are practically the same. Lower A_{\parallel} and higher g_{\parallel} values are usually observed when copper(II) complexes undergo a strong tetrahedral distortion or when five-coordinated adducts with square-pyramidal stereochemistry form.^{59,60} In the present case, the similarity between the g_{\parallel} values suggests that the two diastereoisomer complexes should have the same coordination environment in the equatorial plane, in keeping with the spectroscopic results: the coordination environment for $[\text{Cu}_2(\text{CDDCar})_2\text{H}_{-2}]$ can be proposed in agreement with that of the analogous diastereoisomeric complex $[\text{Cu}_2(\text{CDLCar})_2\text{H}_{-2}]$ ⁴² and with the crystallographic data of the LCar dimeric complex.⁶¹ In the dimeric complexes of

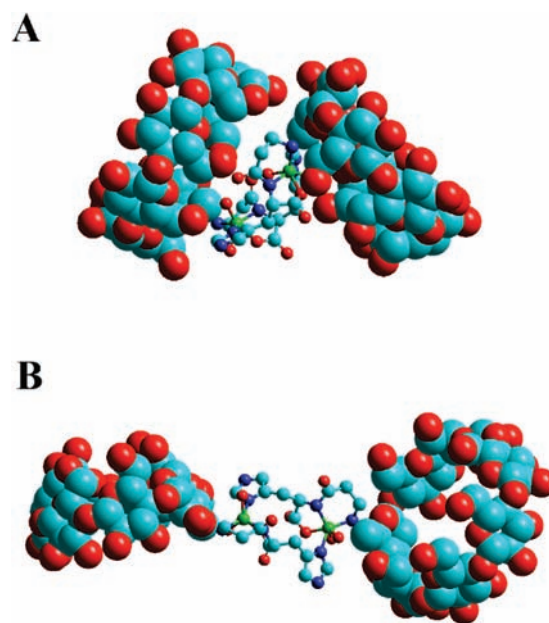
Table 4. Simulated EPR Parameters of Copper(II) Dimeric Species with LCar and DCar Derivatives of CD and Trehalose

species	R (Å)	g_{\parallel}	g_{\perp}	$A_{\parallel} (\times 10^{-4} \text{ cm}^{-1})$	$A_{\perp} (\times 10^{-4} \text{ cm}^{-1})$
$[\text{Cu}_2(\text{CDLCar})_2\text{H}_{-2}]^{42}$	5.1	2.250	2.036	162	26
$[\text{Cu}_2(\text{CDDCar})_2\text{H}_{-2}]$	5.1	2.255	2.045	172	25
$[\text{Cu}_2(\text{TrLCar})_2\text{H}_{-2}]$	5.0	2.260	2.040	163	22
$[\text{Cu}_2(\text{TrDCar})_2\text{H}_{-2}]$	5.1	2.255	2.042	170	23

**Figure 5.** Structures proposed for the $\text{Cu}_2\text{L}_2\text{H}_{-2}$ species of CDDCar.

CDDCar, each metal-ion coordinates amino, amide nitrogen, and carboxylate oxygen of one molecule of CDDCar and is bonded to the second molecule of the ligand by imidazole 3-nitrogen coordination. The ligands in the dimeric structure have a head-to-tail orientation (Figure 5). The slightly higher g_{\perp} and lower A_{\parallel} values are an indication of some kind of apical perturbation, as reported for analogous systems.⁵²

The EPR simulation was extended to similar copper(II) dimeric complexes with LCar and DCar derivatives of the disaccharide trehalose (TrLCar and TrDCar) with the aim of understanding the metal coordination differences between $[\text{Cu}_2(\text{CDLCar})_2\text{H}_{-2}]$ and $[\text{Cu}_2(\text{CDDCar})_2\text{H}_{-2}]$. Both of these dimeric species are characterized by markedly different $\log \beta$ values (8.83 vs 5.23),⁴⁵ as was found for the analogous complex systems with the present derivatives. The magnetic parameters calculated for such metal copper(II) complexes are reported in Table 4. The g_{\parallel} , g_{\perp} , and A_{\perp} values are practically the same for the two diastereoisomer complexes, while the A_{\parallel} value of $[\text{Cu}_2(\text{TrLCar})_2\text{H}_{-2}]$ is lower than that of $[\text{Cu}_2(\text{TrDCar})_2\text{H}_{-2}]$. Consequently, some sort of apical perturbation can be proposed in keeping with the different stability of the dimeric species. For the trehalose derivatives, the different stability of the two copper(II) dimeric species (Table 4) was ascribed to weak interactions, resulting from a larger number of hydrogen bonds as well as from the more effective $\text{CH}-\pi$ interactions occurring in $[\text{Cu}_2(\text{TrLCar})_2\text{H}_{-2}]$.⁴⁵ This causes the dimeric structures of the copper(II) complexes with TrLCar and TrDCar to adopt different conformational states, driven by the histidine stereocenter. By analogy, such weak interactions might be responsible for the different stabilities shown by the copper(II) dimeric species with CDLCar and CDDCar. The hydrophobic CD cavity may also influence the metal coordination environment. Copper(II) complexes with functionalized CDs have been reported to experience interaction with the cavity with a consequent “stiffening” effect that modifies the metal coordination geometry of the copper(II) complex systems in comparison to the underivatized ligands.^{42,52,62} It was demonstrated that the distance of the water molecules coordinated in the apical position is shorter than that the analogous copper(II) complex system without the CD moiety, and this may result from either an interaction of the water molecule with the cavity or even from its replacement by a hydroxymethyl group.

**Figure 6.** Optimized structures of $[\text{Cu}_2(\text{CDLCar})_2\text{H}_{-2}]$ (A) and $[\text{Cu}_2(\text{CDDCar})_2\text{H}_{-2}]$ (B).

In the present case, both $[\text{Cu}_2(\text{CDLCar})_2\text{H}_{-2}]$ and $[\text{Cu}_2(\text{CDDCar})_2\text{H}_{-2}]$ possess two CD units, which may, however, be arranged in a different manner. Molecular modeling led to the optimized structures shown in Figure 6. They support the different conformational arrangement of the CD moieties in the two dimeric species: $[\text{Cu}_2(\text{CDLCar})_2\text{H}_{-2}]$ shows a “compact form” (Figure 6A), while $[\text{Cu}_2(\text{CDDCar})_2\text{H}_{-2}]$ has an “elongated form” (Figure 6B). This would account for the slightly higher distortion found for the copper(II)–CDLCar diastereoisomer (A_{\parallel} values are 162 vs 172 for $[\text{Cu}_2(\text{CDLCar})_2\text{H}_{-2}]$ and $[\text{Cu}_2(\text{CDDCar})_2\text{H}_{-2}]$, respectively). Moreover, the smaller average distance between the CD moieties in the “compact form” should positively influence the number of weak interactions, as was found for similar supramolecular assemblies for which the proximity of CD units has been shown to favor the formation of intermolecular contacts.^{63–65} This likely accounts for the larger stability of the metal dimeric species of the LCar derivative (Figure 6A).

CONCLUSION

The study of the metal binding properties of small peptides, which possess potential therapeutic application, has a central role in the development of clinical approaches directed toward the treatment of metal-involving pathologies. The use of DCar, the enantiomer of the natural dipeptide LCar, has been proposed for the treatment or prevention of oxidative stress-induced disorders because it maintains the same quenching activity of LCar in vitro but is not hydrolyzed by carnosinases. The functionalization of

DCar with a β -CD unit has the purpose of enhancing the bioavailability of the dipeptide by improving the site-specific transport to several tissues.

The investigation of the copper(II) binding properties of the new DCar derivative surprisingly revealed a pronounced difference from the analogous LCar derivative, especially concerning the dimeric species. The spectroscopic data show that this stereoselectivity is driven by noncovalent interactions, namely, hydrogen bonds, CH– π interactions, and steric and hydrophobic effects of the CD cavity.

To the best of our knowledge, these are the first data ever reported on the stereoselectivity of copper(II) complexes with CD–peptide conjugates.

■ ASSOCIATED CONTENT

Supporting Information. ^1H , COSY, TOCSY, and TROESY NMR spectra. This material is available free of charge via the Internet at <http://pubs.acs.org>.

■ AUTHOR INFORMATION

Corresponding Author

*E-mail: gr.vecchio@unict.it. Tel.: +39-095-738-5064. Fax: +39-095-580138.

■ ACKNOWLEDGMENT

We thank Flamma SpA (Bergamo, Italy) for kindly supplying DCar and MIUR (Grants 2008R23Z7K and F5A3AF005) for financial support.

■ REFERENCES

- (1) Severin, K.; Bergs, R.; Beck, W. *Angew. Chem., Int. Ed.* **1998**, *37*, 1634–1654.
- (2) Peacock, A. F.; Iranzo, O.; Pecoraro, V. L. *Dalton Trans.* **2009**, 2271–2280.
- (3) Sovago, I.; Osz, K. *Dalton Trans.* **2006**, 3841–3854.
- (4) Inomata, Y.; Yamaguchi, T.; Tomita, A.; Yamada, D.; Howell, F. S. *J. Inorg. Biochem.* **2005**, *99*, 1611–1618.
- (5) Berthon, G. *Handbook of metal-ligand interactions in biological fluids. Bioinorganic chemistry*; Marcel Dekker: New York, 1995; Vol. 1, p 620.
- (6) Milardi, D.; Rizzarelli, E. *Neurodegeneration: Metallostatics and Proteostasis*; RSC Publishing: Cambridge, U.K., 2011; in press.
- (7) Perez, L. R.; Franz, K. J. *Dalton Trans.* **2010**, *39*, 2177–2187.
- (8) Quinn, P. J.; Boldyrev, A. A.; Formazuyk, V. E. *Mol. Aspects Med.* **1992**, *13*, 379–444.
- (9) Decker, E. A.; Livisay, S. A.; Zhou, S. *Biochemistry (Moscow)* **2000**, *65*, 766–770.
- (10) Kang, J. H.; Kim, K. S.; Choi, S. Y.; Kwon, H. Y.; Won, M. H.; Kang, T.-C. *Mol. Cells* **2002**, *13*, 498–502.
- (11) Hipkiss, A. R.; Worthington, V. C.; Himsforth, D. T. J.; Herwig, W. *Biochim. Biophys. Acta* **1998**, *1380*, 46–54.
- (12) Nagasawa, T.; Yonekura, T.; Nishizawa, N.; Kitts, D. D. *Mol. Cell. Biochem.* **2001**, *225*, 29–34.
- (13) Kohen, R.; Yamamoto, Y.; Cundy, K. C.; Ames, B. N. *Proc. Natl. Acad. Sci. U.S.A.* **1988**, *85*, 3175–3179.
- (14) Cuzzocrea, S.; Genovese, T.; Failla, M.; Vecchio, G.; Fruciano, M.; Mazzon, E.; Di Paola, R.; Muia, C.; La Rosa, C.; Crimi, N.; Rizzarelli, E.; Vancheri, C. *Am. J. Physiol. Lung Cell. Mol. Physiol.* **2007**, *292*, L1095–L1104.
- (15) Fouad, A. A.; El-Rehany, M. A.-A.; Maghraby, H. K. *Eur. J. Pharmacol.* **2007**, *572*, 61–68.
- (16) Ferrari, C. K. B. *Bogerontology* **2004**, *5*, 275–290.
- (17) Calabrese, V.; Cornelius, C.; Mancuso, C.; Pennisi, G.; Calafato, S.; Bellia, F.; Bates, T. E.; Giuffrida Stella, A. M.; Schapira, T.; Dinkova Kostova, A. T.; Rizzarelli, E. *Neurochem. Res.* **2008**, *33*, 2444–2471.
- (18) Shytle, R. D.; Ehrhart, J.; Tan, J.; Vila, J.; Cole, M.; Sanberg, C. D.; Sanberg, P. R.; Bickford, P. C. *Rejuvenation Res.* **2007**, *10*, 173–178.
- (19) Hipkiss, A. R. *Adv. Food Nutr. Res.* **2009**, *57*, 87–154.
- (20) Baran, E. J. *Biochemistry (Moscow)* **2000**, *65*, 789–797.
- (21) Fu, Q.; Dai, H.; Hu, W.; Fan, Y.; Shen, Y.; Zhang, W.; Chen, Z. *Cell. Mol. Neurobiol.* **2008**, *28*, 307–316.
- (22) Trombley, P. Q.; Horning, M. S.; Blakemore, L. J. *Biochemistry (Moscow)* **2000**, *65*, 807–816.
- (23) Barnham, K. J.; Bush, A. I. *Curr. Opin. Chem. Biol.* **2008**, *12*, 222–228.
- (24) Katayama, S.; Nishizawa, K.; Hirano, M.; Yamamura, S.; Momose, Y. *J. Pharm. Pharm. Sci.* **2000**, *3*, 114–117.
- (25) Matsukura, T.; Tanaka, H. *Biochemistry (Moscow)* **2000**, *65*, 817–823.
- (26) Jackson, M. C.; Kucera, C. M.; Lenney, J. F. *Clin. Chim. Acta* **1991**, *196*, 193–205.
- (27) Bellia, F.; Calabrese, V.; Guarino, F.; Cavallaro, M.; Cornelius, C.; De Pinto, V.; Rizzarelli, E. *Antioxid. Redox Signaling* **2009**, *11*, 2759–2775.
- (28) Teufel, M.; Saudek, V.; Ledig, J.-P.; Bernhardt, A.; Boularand, S.; Carreau, A.; Cairns, N. J.; Carter, C.; Cowley, D. J.; Duverger, D.; Ganzhorn, A. J.; Guenet, C.; Heintzelmann, B.; Laucher, V.; Sauvage, C.; Smirnova, T. *J. Biol. Chem.* **2003**, *278*, 6521–6531.
- (29) Lenney, J. F.; Peppers, S. C.; Kucera-Orallo, C. M.; George, R. P. *Biochem. J.* **1985**, *228*, 653–660.
- (30) Otani, H.; Okumura, N.; Hashida-Okumura, A.; Nagai, K. *J. Biochem. (Tokyo)* **2005**, *137*, 167–175.
- (31) Babizhayev, M. A.; Guiotto, A.; Kasus-Jacobi, A. *J. Drug Targeting* **2009**, *17*, 36–63.
- (32) Bertinaria, M.; Rolando, B.; Giorgis, M.; Montanaro, G.; Guglielmo, S.; Buonsanti, M. F.; Carabelli, V.; Gavello, D.; Daniele, P. G.; Fruttero, R.; Gasco, A. *J. Med. Chem.* **2011**, *54*, 611–621.
- (33) Pean, C.; Creminon, C.; Wijkhuizen, A.; Grassi, J.; Guenet, P.; Jehan, P.; Dalbiez, J.-P.; Perly, B.; Djedaini-Pilard, F. *J. Chem. Soc., Perkin Trans. 2* **2000**, 853–863.
- (34) Schaschke, N.; Fiori, S.; Weyher, E.; Escriet, C.; Fourmy, D.; Mueller, G.; Moroder, L. *J. Am. Chem. Soc.* **1998**, *120*, 7030–7038.
- (35) Bjerre, J.; Rousseau, C.; Marinescu, L.; Bols, M. *Appl. Microbiol. Biotechnol.* **2008**, *81*, 1–11.
- (36) Bellia, F.; La Mendola, D.; Pedone, C.; Rizzarelli, E.; Saviano, M.; Vecchio, G. *Chem. Soc. Rev.* **2009**, *38*, 2756–2781.
- (37) van de Manacker, F.; Vermonden, T.; van Nostrum, C. F.; Hennink, W. E. *Biomacromolecules* **2009**, *10*, 3157–3175.
- (38) Wenz, G.; Strassnig, C.; Thiele, C.; Engelke, A.; Morgenstern, B.; Hegetschweiler, K. *Chemistry* **2008**, *14*, 7202–7211.
- (39) Laza-Knoerr, A. L.; Gref, R.; Couvreur, P. *J. Drug Targeting* **2010**, *18*, 645–656.
- (40) Loftsson, T.; Brewster, M. E. *J. Pharm. Pharmacol.* **2010**, *62*, 1607–1621.
- (41) Davis, M. E.; Brewster, M. E. *Nat. Rev. Drug Discovery* **2004**, *3*, 1023–1035.
- (42) Bonomo, R. P.; Bruno, V.; Conte, E.; De Guidi, G.; La Mendola, D.; Maccarrone, G.; Nicoletti, F.; Rizzarelli, E.; Sortino, S.; Vecchio, G. *Dalton Trans.* **2003**, 4406–4415.
- (43) Mineo, P.; Vitalini, D.; La Mendola, D.; Rizzarelli, E.; Scamporrino, E.; Vecchio, G. *J. Inorg. Biochem.* **2004**, *98*, 254–265.
- (44) La Mendola, D.; Sortino, S.; Vecchio, G.; Rizzarelli, E. *Helv. Chim. Acta* **2002**, *85*, 1633–1643.
- (45) Grasso, G. I.; Arena, G.; Bellia, F.; Maccarrone, G.; Parrinello, M.; Pietropaolo, A.; Vecchio, G.; Rizzarelli, E. *Chem.–Eur. J.*, in press.
- (46) Lanza, V.; Bellia, F.; D'Agata, R.; Grasso, G.; Rizzarelli, E.; Vecchio, G. *J. Inorg. Biochem.* **2011**, *105*, 181–188.

- (47) Bellia, F.; Amorini, A. M.; La Mendola, D.; Vecchio, G.; Tavazzi, B.; Giardina, B.; Di Pietro, V.; Lazzarino, G.; Rizzarelli, E. *Eur. J. Med. Chem.* **2008**, *43*, 373–380.
- (48) Boldyrev, A.; Bulygina, E.; Leinsoo, T.; Petrushanko, I.; Tsubone, S.; Abe, H. *Comp. Biochem. Physiol., Part B: Biochem. Mol. Biol.* **2004**, *137*, 81–88.
- (49) Vistoli, G.; Orioli, M.; Pedretti, A.; Regazzoni, L.; Canevotti, R.; Negrisoli, G.; Carini, M.; Aldini, G. *ChemMedChem* **2009**, *4*, 967–975.
- (50) Aldini, G.; Canevotti, R.; Negrisoli, G. U.S. Patent 0,194,493, Aug 14, 2008.
- (51) Flaschka, H. A. *EDTA titrations; an introduction to theory and practice*; Pergamon Press: New York, 1959.
- (52) Bonomo, R. P.; Cucinotta, V.; D'Alessandro, F.; Impellizzeri, G.; Maccarrone, G.; Vecchio, G.; Rizzarelli, E. *Inorg. Chem.* **1991**, *30*, 2708–2713.
- (53) Gran, G. *Analyst* **1952**, *77*, 661–671.
- (54) Gans, P.; Sabatini, A.; Vacca, A. *J. Chem. Soc., Dalton Trans.* **1985**, 1195–2000.
- (55) Smith, T. D.; Pilbrow, J. R. *Coord. Chem. Rev.* **1974**, *13*, 173–278.
- (56) Puglisi, A.; Rizzarelli, E.; Vecchio, G.; Iacovino, R.; Benedetti, E.; Pedone, C.; Saviano, M. *Biopolymers* **2009**, *91*, 1227–1235.
- (57) Sandow, M.; Easton, C. J.; Lincoln, S. F. *Aust. J. Chem.* **1999**, *52*, 1151–1155.
- (58) Haskard, C. A.; Easton, C. J.; May, B. L.; Lincoln, S. F. *Inorg. Chem.* **1996**, *35*, 1059–1064.
- (59) Wayland, B. B.; Kapur, V. K. *Inorg. Chem.* **1974**, *13*, 2517–2520.
- (60) Yokoi, H.; Addison, A. W. *Inorg. Chem.* **1977**, *16*, 1341–1349.
- (61) Freeman, H. C.; Szymanski, J. T. *Acta Crystallogr.* **1967**, *22*, 406–417.
- (62) Bellia, F.; La Mendola, D.; Maccarrone, G.; Mineo, P.; Vitalini, D.; Scamporrino, E.; Sortino, S.; Vecchio, G.; Rizzarelli, E. *Inorg. Chim. Acta* **2007**, *360*, 945–954.
- (63) Frago, A.; Baratto, M. C.; Diaz, A.; Rodriguez, Y.; Pogni, R.; Basosi, R.; Cao, R. *Dalton Trans.* **2004**, 1456–1460.
- (64) Carmona, T.; Gonzalez-Alvarez, M. J.; Mendicuti, F.; Tagliapietra, S.; Martina, K.; Cravotto, G. *J. Phys. Chem. C* **2010**, *114*, 22431–22440.
- (65) Baudel, V.; Landy, D.; Surpateanu, G. *Supramol. Chem.* **2009**, *21*, 442–449.